Articles

Preparation and Proton Conductivity of Sulfonated Polymer-Modified Sintered and Self-Assembled Silica Colloidal Crystals

Joanna J. Smith and Ilya Zharov*

Department of Chemistry, University of Utah, Salt Lake City, Utah 84112

Received July 30, 2008. Revised Manuscript Received February 16, 2009

We prepared sintered self-assembled nanoporous silica colloidal crystals modified with poly(3-sulfopropyl-methacrylate) and poly(stryrenesulfonic acid) brushes covalently attached to the nanopore surface. The resulting robust membranes possess temperature and humidity-dependent proton conductivity of $\sim 2 \times 10^{-2}$ S cm^{-1} at 30 °C and 94% RH, $\sim 1 \times 10^{-2}$ S cm^{-1} at 85 °C and 60% RH, and water uptake of approximately 20 wt % at room temperature. We also prepared proton conductive membranes by self-assembly of silica nanospheres modified with poly(3-sulfopropylmethacrylate) and poly(stryrene-sulfonic acid) brushes of different thickness. These membranes showed a slightly higher proton conductivity and water uptake but poor mechanical properties.

Introduction

Silica colloidal crystals form via self-assembly of silica nanospheres and contain ordered arrays of three-dimensional interconnected nanopores[1] whose surface modification is facile.[2] Thus, they constitute an easy-to-obtain ordered nanoporous material with numerous potential applications. In the past four years, we reported the preparation and molecular transport studies for colloidal films surface-modified with amines,[3,4] polymer brushes,[5,6] chiral selector moieties,[7,8] and suspended colloidal crystals.[9] These studies could lead to applications of surface-modified colloidal crystals in separations and sensing.

Another area of current interest is the preparation and study of proton conductive materials that are the key components of the fuel cell.[10] Polymer electrolyte membranes (PEMs) are the most commonly used proton conducting materials.[11] However, they must be heavily hydrated to transport protons at high rates,[12−14] a condition which is difficult to achieve at elevated temperatures desired for fuel cells operation. As free water is removed from an acidic aqueous electrolyte by heating, ion solvation becomes difficult and protons become localized near their conjugate bases. This process, combined with a gradual loss of connectivity among ion-rich clusters that exist in most PEM materials, causes the very precipitous drop in conductivity with increasing temperature and diminished humidity that is characteristic of nearly all known PEM materials.[14−17] Methanol permeation and swelling in methanol and water[18] also limit the fuel cell operation to the narrow temperature range. To overcome these limitations, thermally stable and nonswelling membranes with high proton conductivity over a wide temperature range are desirable.[19]

A recent approach to proton conductive materials is to prepare organic−inorganic composites.[20,21] Nanocomposite membranes where inorganic oxide nanoparticles are dispersed inside a polyelectrolyte received the most attention so far. The nanoparticles are hydrophilic and therefore help to retain moisture inside the membrane at high temperature.

(1) Wong, S.; Kitaev, V.; Ozin, G. A. *J. Am. Chem. Soc.* **2003**, *125*, 15589–15598.
(2) Onclin, S.; Ravoo, B. J.; Reinhoudt, D. N. *Angew. Chem., Int. Ed.* **2005**, *44*, 6282–6304.
(3) Newton, M. R.; Bohaty, A. K.; White, H. S.; Zharov, I. *J. Am. Chem. Soc.* **2005**, *127*, 7268–7269.
(4) Newton, M. R.; Bohaty, A. K.; Zhang, Y.; White, H. S.; Zharov, I. *Langmuir* **2006**, *22*, 4429–4432.
(5) Schepelina, O.; Zharov, I. *Langmuir* **2006**, *22*, 10523–10527.
(6) Schepelina, O.; Zharov, I. *Langmuir* **2007**, *23*, 12704–12709.
(7) Cichelli, J.; Zharov, I. *J. Am. Chem. Soc.* **2006**, *128*, 8130–8131.
(8) Cichelli, J.; Zharov, I. *J. Mater. Chem.* **2007**, *17*, 1870–1875.
(9) Bohaty, A. K.; Zharov, I. *Langmuir* **2006**, *22*, 5533–5536.
(10) Winter, M.; Brodd, R. J. *Chem. Rev.* **2004**, *104*, 4245–4269.
(11) Gary, F. M. *Polymer Electrolytes*; Royal Society of Chemistry: Cambridge, 1997.
(12) Zawodzinski, T. A., Jr.; Springer, T. E.; Uribe, F.; Gottesfeld, S. *Solid State Ionics* **1993**, *60*, 199–211.
(13) Cappadonia, M.; Erning, J. W.; Stimming, U. *J. Electroanal. Chem.* **1994**, *376*, 189–193.
(14) Mauritz, K. A.; Moore, R. B. *Chem. Rev.* **2004**, *104*, 4535–4585.
(15) Yeo, R. S.; Cheng, C. H. *J. Appl. Polym. Sci.* **1986**, *32*, 5733–5741.
(16) Hickner, M. A.; Ghassemi, H.; Kim, Y. S.; Einsla, B. R.; McGrath, J. E. *Chem. Rev.* **2004**, *104*, 4587–4611.
(17) Li, Q.; He, R.; Jensen, J. O.; Bjerrum, N. J. *Chem. Mater.* **2003**, *15*, 4896–4915.
(18) Yeo, S. C.; Eisenberg, A. *J. Appl. Polym. Sci.* **1977**, *21*, 875–898.
(19) Dresselhaus, M.; Crabtree, G.; Buchanan, M. *Basic Research Needs for the Hydrogen Economy. A Report on the Basic Energy Sciences Workshop on Hydrogen Production, Storage, and Use*; Argonne National Laboratory, U.S. Department of Energy: Chicago, 2004; pp 1−178.
(20) Costamagna, P.; Yang, C.; Bocarsly, A. B.; Srinivasan, S. *Electrochim. Acta* **2002**, *47*, 1023–1033.
(21) Valle, K.; Belleville, P.; Pereira, F.; Sanchez, C. *Nat. Mater.* **2006**, *5*, 107–111.

10.1021/cm8020929 CCC: $40.75
Published on Web 04/30/2009

The added nanoparticles increase moisture content, mechanical, thermal, and chemical stability, and proton conductivity of the composite membrane enough to compete with Nafion performance.[22−24] In addition, nanocomposite membranes showed lower methanol permeability.[25,27,35] The commonly used inorganic nanoparticles are oxides (SiO_2, Al_2O_3, TiO_2, ZrO_2),[26−28] clays,[29] or zeolites.[30,31] Membranes containing in situ grown colloidal silica[32,33] and inorganic powder-gel composites[34,35] have also been reported. Finally, silica matrices filled with polyelectrolytes have also been prepared[36−39] and showed the proton conductivity in the range of $10^{-4}-10^{-2}$ S/cm, low methanol permeability, and good mechanical properties.

We decided to explore another approach to hybrid proton-conducting membranes, in which the highly ordered silica colloidal crystal serves as a matrix containing a continuous network of nanopores providing mechanical stability and water retention, while surface-bound polymer brushes carrying acidic groups provide the proton conductivity. Our design has a number of features that distinguish it from polyelectrolyte or composite organic−inorganic membranes, relying on the polymer phase for both the mechanical stability and the proton conductivity. The matrix eliminates the need to simultaneously optimize the mechanical and proton-conducting properties of the polymer and thus allows introducing and investigating unprecedented polymer brush architectures prepared by surface-initiated living polymerization inside the inorganic nanopores. This polymerization technique guarantees that the covalently attached polyelectrolytes will not leach out of the nanopores. In addition, the inorganic matrix allows achieving high degrees of acid functionalization of the polymer without the danger for the membrane to become water-soluble and maintaining mechanical stability under oxidative conditions and high temperature.

The notions of the structural order and nanopore continuity in the colloidal crystal matrix may be particularly important. Indeed, it is known that the proton conductivity of PEMs is enhanced by nanoscale phase separation of ionic and nonionic domains into bicontinuous structures.[40,41] Most of the materials studied contained randomly distributed polymeric domains or nanopores (in the case of the composite materials). However, there are some indications that order is important. Ordered mesoporous materials showed high proton conductivity.[42−45] Recently, we described the transport of protons across the surface in free-standing assemblies of surface-sulfonated silica nanospheres both randomly packed and self-assembled into a close-packed arrangement[46] and demonstrated that their proton conductivity depends on the ordering of the material, where the increase in structural organization of the self-assembled colloidal materials led to increased proton conductivity and better water retention. In addition, it has been shown that high proton conductivity observed in self-assembled surface-charged latex nanoparticle films results from the presence of continuous charged hydrophilic channels that form during self-assembly of the particles.[47] Finally, having a highly ordered material greatly facilitates its computational modeling, which is particularly important given the current lack of understanding of the structural factors influencing the proton conductivity.

Thus, the main purpose of the work presented here is to examine the feasibility of nanopore surface modification in the recently reported sintered silica colloidal crystals[48] with sulfonated polymer brushes. The study of the proton conductivity and water retention for these materials would allow evaluating our novel design. As an additional evaluation method we decided to compare the polymer-modified sintered colloidal crystals to self-assembled colloidal crystals prepared using silica nanospheres carrying sulfonated polymer brushes. This work is presented as a proof-of-principle for the novel material design, and thus long-term stability, methanol permeability, and fuel cell performance characteristics of the material will be reported elsewhere.

Experimental Section

Materials. Tetraethyl orthosilicate (TEOS) (99+%, Alfa Aesar) was used as received. 3-Sulfopropylmethacrylate, potassium salt (SPM) (98%), 4-styrenesulfonic acid, sodium salt (SSA), 3-aminopropyltriethoxy-silane (APTES) (99%), 2-bromoisobutyryl bromide (98%), copper(I) chloride (99.995+%), copper(II) chloride (99.999%), copper(I) bromide (99.999%), 2,2′-dipyridyl (Bipy)

(22) Chang, J. H.; Park, J. H.; Park, G. G.; Kim, C. S.; Park, O. O. *J. Power Sources* **2003**, *124*, 18–25.
(23) Bhattacharyya, A. J.; Maier, J. *Adv. Mater.* **2004**, *16*, 811–814.
(24) Beyazyildirim, S.; Kreuer, K. D.; Schuster, M.; Bhattacharyya, A. J.; Maier, J. *Adv. Mater.* **2008**, *20*, 1274–1278.
(25) Navarra, M. A.; Materazzi, S.; Panero, S.; Scrosati, B. *J. Electrochem. Soc.* **2003**, *150*, A1528−A1532.
(26) Watanabe, M.; Uchida, H.; Igarashi, H. *Macromol. Symp.* **2000**, *156*, 223–230.
(27) Satolli, D.; Navarra, M. A.; Panero, S.; Scrosati, B.; Ostrovski, D.; Jacobsson, P.; Albinsson, I.; Mellander, B.-E. *J. Electrochem. Soc.* **2003**, *150*, A267−A273.
(28) Hamoudi, S.; Kaliaguine, S. *Micropor. Macropor. Mater.* **2003**, *59*, 195–204.
(29) Wang, J.; Merino, J.; Aranda, P.; Galvan, J.-C.; Hitzky-Ruiz, E. *J. Mater. Chem.* **1999**, *9*, 161–167.
(30) Kwak, S. H.; Yang, T. H.; Kim, C. S.; Yoon, K. H. *Electrochim. Acta* **2004**, *50*, 653–657.
(31) Tricoli, V.; Nannetti, F. *Electrochim. Acta* **2003**, *48*, 2625–2633.
(32) Zoppi, A.; Yoshida, I. V. P.; Nunes, S. P. *Polymer* **1998**, *39*, 1309–1315.
(33) Mauritz, K. A. *Mater. Sci. Eng.* **1998**, *6*, 121–133.
(34) Peled, E.; Duvdevani, T.; Melman, A. *Solid State Lett.* **1998**, *1*, 210–211.
(35) Peled, E.; Duvdevani, T.; Aharon, A.; Melman, A. *Electrochem. Solid State Lett.* **2000**, *3*, 525–528.
(36) Mitsui, T.; Morikawa, H.; Kanamura, K. *Electrochemistry* **2002**, *70*, 934–936.
(37) Munakata, H.; Chiba, H.; Kanamura, K. *Solid State Ionics* **2005**, *176*, 2445–2450.
(38) Kanamura, K.; Mitsui, T.; Munakata, H. *Chem. Mater.* **2005**, *17*, 4845–4851.
(39) Zhang, X. *J. Elctrochem. Soc.* **2007**, *154*, B322−B326.
(40) Yeager, H. L. In *Transport Properties of Perfluorosulfonate Polymer Membranes in Perfluorinated Ionomer Membranes*; ACS Symposium Series; Eisenberg, A., Yeager, H. L., Eds.; American Chemical Society: Washington, DC, 1982; Vol. 180; p 49.
(41) Rubatat, L.; Rollet, A. L.; Gebel, G.; Diat, O. *Macromolecules* **2002**, *35*, 4050.
(42) Yamada, M.; Li, D.; Honma, I.; Zhou, H. *J. Am. Chem. Soc.* **2005**, *127*, 13092–13093.
(43) Li, H.; Nogami, M. *Adv. Mater.* **2002**, *14*, 912–914.
(44) Marschall, R.; Rathouský, J.; Wark, M. *Chem. Mater.* **2007**, *19*, 6401–6407.
(45) Sasajima, K.; Munakata, H.; Kanamura, K. *J. Electrochem. Soc.* **2008**, *155*, B143−B147.
(46) Smith, J. J.; Zharov, I. *J. Mater. Chem.* **2008**, *18*, 5335–5338.
(47) Gao, J.; Lee, D.; Yang, Y.; Holdcroft, S.; Frisken, B. J. *Macromolecules* **2005**, *38*, 5854–5856.
(48) Bohaty, A. K.; Smith, J. J.; Zharov, I. *Langmuir* **2009**, ASAP.

(ReagentPlus ≥99%), and tetrabutylammonium hydroxide (40 wt % solution in water) were obtained from Aldrich and used as received. 4-Dimethyl-aminopyridine (DMAP) (≥98.0%, Fluka) was used as received. Silver Print II (GC Electronics) was used to coat the colloidal membranes for EIS measurements (see below).

Preparation and Modification of Silica Nanoparticles. Silica spheres were synthesized using the Stöber method,[49] by adding 0.2 M tetraethyl orthosilicate (TEOS) in absolute ethanol to a solution of 0.4 M ammonia and 17 M water in absolute ethanol. The mixture was stirred for 24 h at room temperature. Silica spheres were collected and purified by repeated centrifugation in absolute ethanol. The diameter of the spheres was determined to be 242.5 ± 23 nm by DLS. Silica spheres with a diameter of 358.2 ± 45 nm were synthesized using the same method except the ammonia concentration was 0.79 M.

Poly(3-sulfopropylmethacrylate) (pSPM) and poly(stryrene-sulfonic acid) (pSSA) brushes were grown onto ∼240 nm initiator-modified silica spheres via atom transfer radical polymerization (ATRP). The synthesis of initiator-modified silica spheres was achieved in two steps. First, the silica nanoparticles (1 g) were suspended in 50 mL of 0.06 M 3-aminopropyltriethoxysilane (APTES) dry acetonitrile solution for 17 h at room temperature. The amine-modified spheres were collected and rinsed with acetonitrile via repeated centrifugation. The amine-functionalized particles (1 g) were then suspended in 50 mL of dry dichloromethane solution of 0.15 M dry triethylamine, 0.13 M 2-bromoisobutyryl bromide, and a catalytic amount of DMAP for 12 h at room temperature. The initiator-modified particles were isolated and rinsed with dichloromethane by centrifugation.

The grafting of pSPM brushes onto the initiator-modified silica spheres (1 g) was carried out in 10 mL of a 2:1 mixture of degassed methanol and water, containing 3-sulfopropyl-methacrylate potassium salt (0.5 M), 2,2′-dipyridyl (0.08 M), $CuCl_2$ (0.006 M), and CuCl (0.02 M) at room temperature. Similarly, the polymerization of pSSA brushes onto initiator-modified silica spheres were carried out in a 2:3 mixture of degassed methanol and water, containing styrenesulfonic acid sodium salt (0.8 M), 2,2′-dipyridyl (0.03 M), and CuBr (0.02 M) at room temperature. The polymerization times were varied from 20 min to 24 h. After polymerization the samples were quenched and rinsed with water. To exchange the potassium and sodium ions with protons, the spheres were soaked in 1 M HCl for one day then rinsed with water to remove any excess acid.

Preparation of Polymer-Modified Silica Membranes. Silica colloidal membranes were prepared by sedimentation of the polymer-modified silica spheres from ∼4 wt % ethanol colloidal solutions followed by solvent evaporation, which worked better than a vertical deposition method. This process resulted in the formation of mechanically robust ∼300 μm thin membranes. Overall, the polymer modified membranes were more robust in comparison to unmodified silica membranes.

Preparation and Modification of Sintered Silica Membranes. Sintered silica colloidal membranes were prepared using the procedure similar to that reported by Wirth et al.[50] Silica spheres of 358 nm in diameter were calcinated at 600 °C for 4 h. After the calcination, the silica sphere diameter decreased to ∼320 nm. Colloidal membranes were then prepared by vertical deposition of ∼12 wt % ethanol colloidal solutions onto a glass substrate, and then the membranes were easily removed from the glass substrate. The resulting membranes, ∼300 μm thick, were sintered in a furnace at 1050 °C for 12 h. The final sintered silica colloidal membranes were very robust and durable. The thickness of the membranes can be controlled by changing the weight percent ethanol colloidal solutions. For instance, larger weight percent solutions result in thicker membranes. We have found that using <8 wt % ethanol colloidal solutions with silica spheres ∼200−300 nm in diameter resulted in very thin membranes that were hard to remove from the glass substrate and would crack easily. Overall, the thinnest membranes we made, composed of ∼300 nm diameter silica spheres, that were durable and crack free, were about ∼200 μm.

The sintered membranes were rehydroxylated in a solution of tetrabutylammonium hydroxide of pH 9.5 at 60 °C for 48 h. The membranes were rinsed with H_2O (100 mL × 2), 1 M nitric acid (100 mL × 2), methanol (100 mL × 2), H_2O (100 mL 2x), and acetonitrile (100 mL × 2). The sintered silica colloidal crystals were then modified with amines by placing the rehydroxylated sintered membranes in 10 mL of 0.05 M APTES dry acetonitrile overnight at room temperature under N_2(g). After modification, the samples were rinsed with acetonitrile, and the amine modification procedure was repeated again. The amine-modified sintered membranes were then placed in 10 mL of dry dichloromethane solution of 0.15 M dry triethylamine, 0.13 M 2-bromoisobutyryl bromide, and a catalytic amount of DMAP and allowed to react overnight at room temperature. The initiator-modified membranes were then rinsed with dichloromethane. The sulfonated polymers were then introduced to the initiator-modified silica membranes via ATRP. The polymerization of pSPM was carried out in enough solution to cover the samples, of a 2:1 mixture of degassed methanol and water, containing 3-sulfopropyl-methacrylate potassium salt (0.7 M), 2,2′-dipyridyl (0.03 M), $CuCl_2$ (0.003 M), and CuCl (0.007 M) at room temperature under N_2(g) for ∼10 h. Similarly, the polymerization of pSSA brushes onto initiator-modified silica spheres were carried out in a 2:3 mixture of degassed methanol and water, containing styrenesulfonic acid sodium salt (0.8 M), 2,2′-dipyridyl (0.03 M), and CuBr (0.02 M) at room temperature under N_2(g) for 10 h. After polymerization the resulting membranes were rinsed with water and soaked overnight in 1 M HCl and then rinsed with water to remove any excess acid.

Characterization. Dynamic light scattering (Nicomp 380 ZLS) was used to perform the size characterization of the polymer-modified silica spheres. Scanning electron microscopy (Hitachi S3000-N) was used to image the colloidal assemblies. Thermogravimetric analysis of polymer-modified silica spheres was performed using TGA Q500 (TA Instruments).

Electrochemical Impedance Spectroscopy Measurements. Silver paint was coated on both sides of the colloidal assemblies to serve as the electrodes. The impedance was measured using a two probe testing device placed in a homemade humidity and temperature controlled chamber. This chamber was built from a vacuum oven that was modified with the components necessary to achieve a controlled relative humidity (RH) environment. The relative humidity was controlled by injecting DI water through a heated inlet tube. The relative humidity and temperature in the oven was measured using a humidity and temperature meter (Vaisala HUMICAP with a HMP77 probe). The complex impedance of the samples was measured using Princeton Applied Research VersaSTAT^3, in the frequency range of 1 MHz to 0.1 Hz. The proton conductivity was calculated using the equation $\sigma = L/RA$, where σ is the ionic conductivity, L is the distance between the two electrodes, R is the resistance of the colloidal material, and A is the cross-sectional area of the material. The proton conductivity values for at least two different membranes made from the same batch of polymer-modified silica spheres were averaged.

(49) Stöber, W.; Fink, A.; Bohn, E. *J. Colloid Interface Sci.* **1968**, *26*, 62–69.
(50) Le, T. V.; Ross, E. E.; Velarde, R. C.; Legg, M. A.; Wirth, M. J. *Langmuir* **2007**, *23*, 8554–8559.

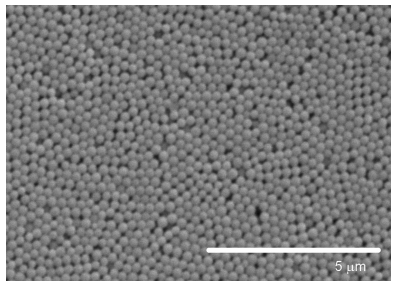

Figure 1. SEM image of sintered silica colloidal crystal comprised of ~300 nm diameter silica nanoparticles. Size bar = 5 μm.

Scheme 1

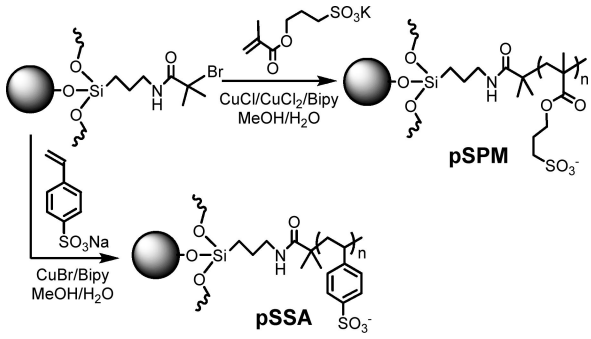

Water Uptake Measurements. The average water uptake of the polymer-modified membranes was calculated as follows:

$$\text{water uptake (\%)} = \frac{W_{\text{wet}} - W_{\text{dry}}}{W_{\text{dry}}} \times 100 \qquad (1)$$

where W_{dry} is the dry weight of the membrane and W_{wet} is the wet weight of the membrane. The dry weights were determined by weighing the membranes after being dried under vacuum at 90 °C overnight, cooled in a desiccator, and weighing immediately. The wet weight of the membranes (not sintered) was determined by weighing the membranes after keeping them in a constant humidity−temperature chamber at 97% R.H. and room temperature for 24 h. The wet weight of the sintered membranes was determined by soaking them in water at room temperature for 24 h, then wiping the samples with filter paper and weighing them immediately.

Results and Discussion

Polymer-Modified Sintered Silica Colloidal Membranes. Figure 1 shows an SEM image of a sintered colloidal crystal, comprised of ~300 nm diameter silica spheres, in which the silica spheres are adhered to one another. As a result of sintering, this material is very robust and durable. The sintered silica colloidal crystals ~300 μm thick and ~1 cm across were modified with pSPM and pSSA sulfonated polymer brushes by surface-initiated ATRP (Scheme 1). TGA was used to characterize the polymer-modified sintered membranes, as shown in Figure 2. After the initiator functionalization, we observed a smooth weight loss, up to 800 °C, of ~1.7% due to the initiator molecules. In contrast, a significant weight loss for the polymer modified silica membranes was observed above 150 °C. Specifically, pSSA (Figure 2) begins to decompose around 250 °C, with a polymer weight loss around 5.8 wt %. The pSPM polymer behaves differently. This polymer is less stable and begins

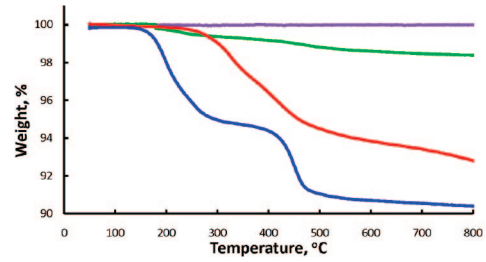

Figure 2. Thermogravimetric analysis (TGA) plots for unmodified (top line, purple), initiator-modified (second line from top, green), pSSA modified, polymerization time = 12 h (third line from top, red), and pSPM modified, polymerization time = 7 h (bottom line, blue) sintered silica colloidal membranes.

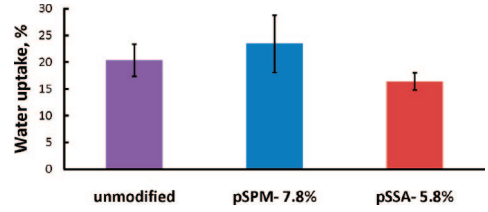

Figure 3. Water uptake for sintered silica membranes after soaking in water at room temperature for 24 h.

to decompose at a lower temperature, ~150 °C, and has two main degradation stages likely due to the polymer backbone and sulfonic acid groups,[51] with an overall polymer weight loss around 7.8 wt %. The molecular weight of the polymers formed inside the colloidal nanopores of the sintered membranes appears to be limited to a maximum polymer chain length (or weight percent) due to the geometrical constraints. Thus, the weight % loss for pSPM membranes levels off at ~8 wt %, and the pSSA membranes levels off at ~6 wt % after 10 h of polymerization.

Water uptake of the sintered membranes (Figure 3) was measured by soaking the membranes in water at room temperature for 24 h and calculated using eq 1. Given that the void fraction of the colloidal crystal is 26%, it appears that both polymers are significantly hydrated, with pSPM being hydrated almost completely and pSSA falling slightly below. The water uptake of pSPM and pSSA sintered silica membranes is lower than that of Nafion (~38% water uptake measured under the same conditions[52]). The sintered polymer-modified membranes did not swell in the course of these experiments.

Next, we measured the proton conductivity of the polymer-modified colloidal membranes using electrochemical impedance spectroscopy. Figure 4A shows the proton conductivity of sintered pSPM and pSSA membranes at 30 and 98 °C as a function of relative humidity. It is clear that both membranes have similar proton conductivities which increase with relative humidity, with a maximum value of ~2×10^{-2} S cm^{-1} achieved at 30 °C and 94% RH. The proton conductivity of the polymer-modified sintered colloidal membranes is affected by temperature, as shown in Figure

(51) Sahu, A. K.; Selvarani, G.; Pitchumani, S.; Sridhar, P.; Shukla, A.; Narayanan, K. N.; Banerjee, A.; Chandrakumarc, N. *J. Electrochem. Soc.* **2008**, *155*, B686−B695.
(52) Pereira, F.; Vallé, K.; Belleville, P.; Morin, A.; Lambert, S.; Sanchez, C. *Chem. Mater.* **2008**, *20*, 1710–1718.

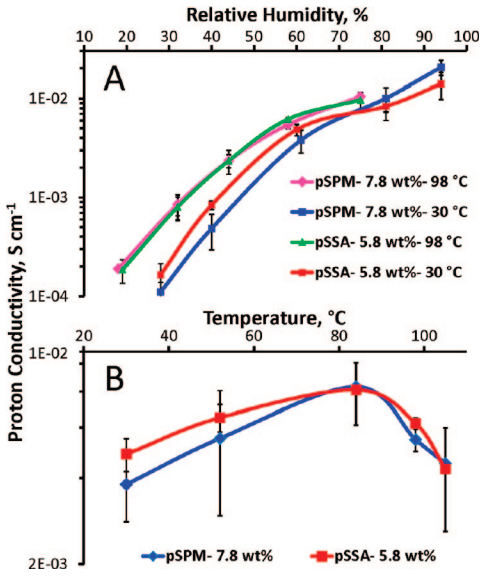

Figure 4. Proton conductivity of pSPM and pSSA sintered colloidal membranes as a function of (A) relative humidity at 30 and 98 °C and (B) temperature at 60% relative humidity.

4B. The proton conductivity for both membranes at 60% RH increases gradually with increasing temperature up to 85 °C and then decreases.

Overall, the proton conductivity values obtained for the sintered polymer-modified colloidal membranes are comparable to those of Nafion. For instance, at room temperature and 30−80% RH Nafion-115 possesses proton conductivity values in the range of 2×10^{-3} to 7×10^{-2} S cm^{-1}.[39] A comparison with proton conductive fully sulfonated polystyrene membranes cannot be made as this polymer is water-soluble. Carretta and co-workers have reported[53] the synthesis, proton conduction, and methanol permeation of membranes based on partially sulfonated polystyrene. The authors studied membranes varied between 10 and 20 mol % sulfonation and did not exceed 20 mol % sulfonation since the material would become too water-soluble. The membranes with 10 mol % sulfonation were rather brittle and stiff while the membranes with 20 mol % sulfonation were flexible even in the dry state. As expected, the most extensively sulfonated membranes had the highest proton conductivity of 5×10^{-2} S cm^{-1} at room temperature in its fully hydrated state.

While the proton conductivity observed for the new materials is quite high, it is lower than expected based on the design with continuous interconnected nanopores. This may result from the intrinsic proton conductivity properties of the sulfonated polymers used in the present work, and thus the conductivity could be further enhanced by using other sulfonated polymers. Combined with the extensive set of other potential advantages (see above), we believe that the new materials presented in the present work are quite attractive and promising.

Self-Assembled Silica Sphere/Sulfonated Polymer Colloidal Membranes. Sulfonated linear polymer brushes, pSPM and pSSA, were grown onto initiator-modified silica spheres via ATRP (Scheme 1). The length of these bushes was controlled by the polymerization time and measured using dynamic light scattering (DLS). The DLS results are shown in Table 1. It is clear that longer polymerization times lead to longer polymer chains, as expected. As shown in Table 1, the polymer brushes were examined in two different solvents, water and acetonitrile. As expected, the polymer brushes appear to be swollen in water, due to the strong repulsive interaction between the neighboring ionized sulfonic acid groups. In contrast, the brushes appear to be in a collapsed state when immersed in acetonitrile.

Table 1. DLS Data for the Polymer-Modified Silica Spheres Immersed in Water and Acetonitrile as a Function of Polymerization Time

		solvent			
		H_2O		CH_3CN	
polymer	polymerization time	d,[b] nm	Δr,[c] nm	d,[b] nm	Δr,[c] nm
pSPM	0[a]	242 ± 23	0	251 ± 27	0
	20 min	321 ± 22	39.5	285 ± 35	17
	2 h	465 ± 90	111.5	317 ± 36	33
	6 h	965 ± 120	361.5	343 ± 36	46
pSSA	1 h	325 ± 41	41.5	295 ± 33	22
	24 h	1214 ± 129	486	426 ± 51	87.5

[a] Initiator modified. [b] Silica sphere diameter. [c] Brush thickness.

Table 2. TGA Data for the Polymer-Modified Silica Spheres as a Function of Polymerization Time

polymer	polymerization time	Total % weight loss	% wt. loss due to polymer
	bare silica spheres	3.5	
	initiator-modified	5.7	
pSPM	20 min	8.4	2.7
	2 h	16.3	10.6
	6 h	41.5	35.8
pSSA	1 h	10.2	4.5
	24 h	27.9	22.2

Thermograviametric analysis was performed for the polymer-modified silica spheres to examine the polymer weight content and the thermal stability of the hybrid organic−inorganic material. The TGA results are shown in Table 2. For the unmodified silica spheres, there was a smooth weight loss up to 800 °C due to drying of the silica spheres, with a total loss of 3.5 wt %. After functionalization of the silica spheres with initiator moieties there was an additional 2.2 wt % loss due to the initiator molecules. The pSSA polymer-modified silica spheres began to decompose around 250 °C, while the pSPM polymers were less stable and started to decompose around 150 °C. Overall, it is clear from the TGA data that longer polymerization times lead to the growth of longer polymer chains.

Next, we prepared self-assembled colloidal membranes using the polymer-modified silica spheres and studied their proton conductivity and water uptake. We used SEM to image the membranes prepared using sedimentation of polymer-modified silica spheres from ethanol onto a glass support. The spheres carried polymer brushes of varying length as determined by DLS in water. The SEM images are shown in Figure 5. For the membranes prepared from the silica spheres carrying short polymer brushes (Figure 5A,C) the individual silica nanoparticles and nanopores are clearly visible. However, the membranes prepared from the

(53) Carreta, N.; Tricoli, V.; Picchioni, F. *J. Membr. Sci.* **2000**, *166*, 189–197.

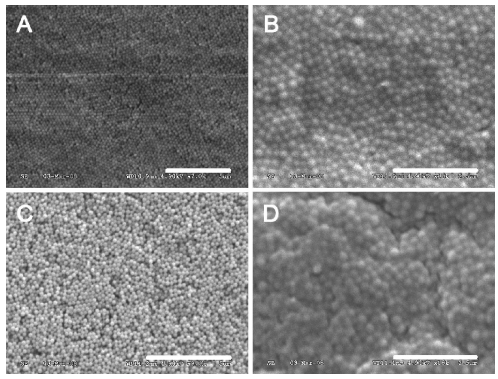

Figure 5. SEM images of (A) pSPM-39.5 nm, (B) pSPM 361.5 nm, (C) pSSA-41.5 nm, and (D) pSSA-486 nm polymer-modified self-assembled silica membranes. Size bars: A, C = 5 μm; B, D = 2.5 μm.

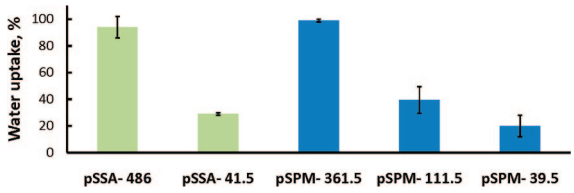

Figure 6. Water uptake of polymer-modified self-assembled silica membranes after keeping membranes in a humidity−temperature controlled chamber at 97% RH and room temperature for 24 h.

silica spheres carrying longer polymer chains (Figure 5B,D) appear as a polymer film, in which the silica spheres are imbedded and held inside due to the polymer brush entanglement. The latter membranes possess polymer-like characteristics, such as flexibility, compared to the stiffer membranes made with shorter polymer brushes. It is interesting to note that the pSPM membranes appear to have better packing and order than the pSSA membranes. This is likely a result of using ethanol, a poor solvent for pSSA polymers, during the membrane assembly where the silica spheres precipitate too rapidly and do not have sufficient time to self-assemble into a closed-packed structure.

We studied the water uptake of the different polymer-modified silica membranes (Figure 6). The average water uptake of the different membranes was calculated using eq 1 after keeping the membranes in a constant humidity−temperature chamber at 97% RH and room temperature for 24 h. It is clear that longer polymer brushes contain more water, with two membranes made using the longest polymer brushes being essentially saturated with water. The water uptake by the self-assembled membranes is significantly higher compared to that for the sintered membranes.

Next, we measured the proton conductivity of the self-assembled sulfonated polymer-modified silica membranes using electrochemical impedance spectroscopy (Figures 7 and 8). For both types of polymer-modified membranes, pSPM and pSSA, there is an increase in proton conductivity with longer polymers, due to an increase in the number of sulfonic acid groups. It is clear from Figures 7A and 8A that both types of polymer-modified membranes, pSPM and pSSA, have comparable proton conductivity values, with a maximum value of $\sim 6 \times 10^{-2}$ S cm^{-1} for both pSPM 361.5 nm and pSSA 486 nm at 98 °C and 70% RH. These values are slightly higher than the proton conductivity values obtained

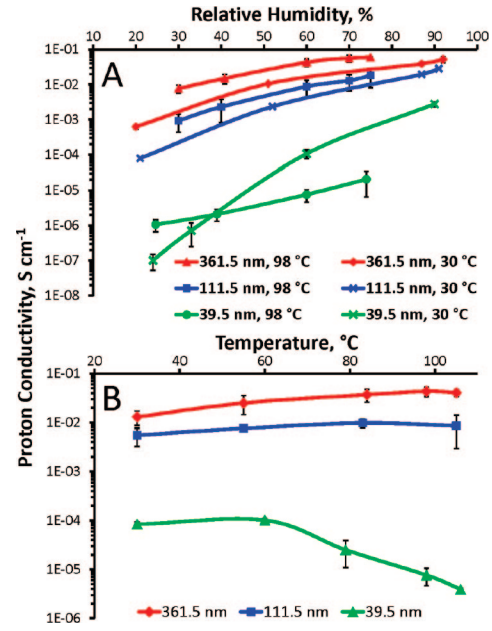

Figure 7. Proton conductivity of pSPM membranes as a function of (A) relative humidity at 30 and 98 °C and (B) temperature at 60% relative humidity.

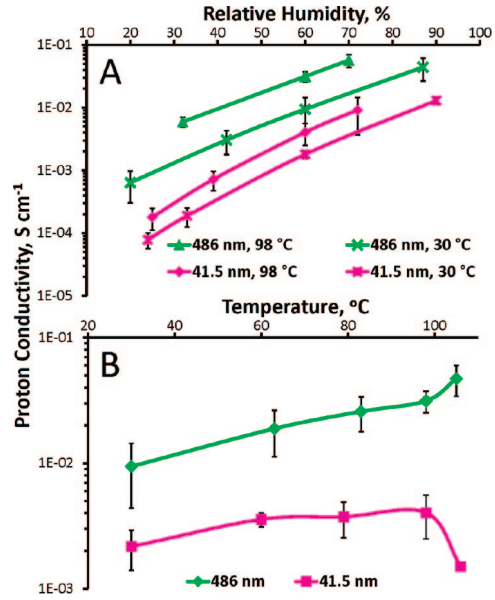

Figure 8. Proton conductivity of pSSA membranes as a function of (A) relative humidity at 30 and 98 °C and (B) temperature at 60% relative humidity.

for the polymer-modified sintered colloidal membranes (see above). The proton conductivity of all the membranes increases with increasing relative humidity, as expected.

The temperature dependence of the proton conductivity at 60% RH for the polymer-modified silica membranes was also examined, as shown in Figures 7B and 8B. The proton conductivity for most of the membranes increases with temperature, except for the pSPM 39.5 nm and pSSA 41.5 nm membranes. These membranes have lower conductivity at higher temperature, most likely due to a small size of the polymer chains, which makes it hard to retain water molecules at higher temperatures. Their proton conductivity is too low for use in any practical applications. In comparison, the other pSPM and pSSA membranes have higher

conductivity values which increase gradually with temperature. The highest conductivity values were 4×10^{-2} S cm^{-1} at 105 °C for pSPM 361.5 nm and 4.7×10^{-2} S cm^{-1} at 105 °C for the pSSA 486 nm membranes at 60% RH.

Overall, we showed that sulfonated polymer-modified silica spheres can self-assemble into membranes that possess high proton conductivity. However, these membranes are brittle when made using the silica spheres carrying short polymer brushes or can fall apart when made using the silica spheres carrying longer polymer brushes due to swelling when immersed in solvents. Therefore, despite their ease of preparation, these membranes are inferior for practical purposes compared to the sintered colloidal membranes.

Conclusions

We demonstrated that sintered self-assembled nanoporous silica colloidal crystals modified with poly(3-sulfopropylmethacrylate) and poly(stryrenesulfonic acid) brushes covalently attached to the nanopore surface possess high proton conductivity and water uptake. Combined with the extensive set of other potential advantages including a continuous network of ordered nanopores with tunable sizes providing mechanical stability and water retention, the ability to optimize the surface-bound polyelectrolyte brush structure, and the mechanical stability of the inorganic matrix, we believe that we provided a proof-of-principle for a novel promising colloid-based proton conductive material. Work is under way to examine the long-term stability and methanol permeability of the novel membranes and to construct fuel cells using these membranes to study their electrochemical performance and to confirm their utility for fuel cell applications. We also prepared proton conductive membranes by self-assembly of silica nanospheres modified with poly(3-sulfo-propylmethacrylate) and poly(stryrenesulfonic acid) brushes of different thicknesses. These membranes showed a slightly higher conductivity and water uptake but poor mechanical properties.

Acknowledgment. This work was supported in part by the NSF NER (CBET-0708368) and ACS PRF (46784-AC 10). We are grateful to Prof. Anil V. Virkar, Dr. Dmitry Bedrov, and Dr. Oleg Borodin (Materials Science and Engineering, University of Utah) for helpful discussions and to Mr. Jason M. Boyle (Chemistry, University of Utah) for his help with assembling the constant humidity chamber.

CM8020929